Transport of Helical Gyrotactic Swimmers in Channels

M. S. Alqarni and R. N. Bearon[a)]

Department of Mathematical Sciences, University of Liverpool, Peach Street, Liverpool, L69 7ZL, UK

(Dated: 30 June 2016)

We develop a mechanistic model that describes the transport of gyrotactic cells with propulsive force and propulsive torque that are not parallel. In sufficiently weak shear this yields helical swimming trajectories, whereas in stronger shear cells can attain a stable equilibrium orientation. We obtain the stable equilibrium solution for cell orientation as a function of the shear strength and determine the feasibility region for equilibrium solutions. We compute numerically the trajectories of cells in two dimensional vertical channel flow where the shear is non-uniform. Depending on the parameter values, we show that helical swimmers may display classical gyrotactic focussing towards the centre of the channel, or can display a new phenomenon of focussing away from the centre of the channel. This result can be explained by consideration of the equilibrium solution for cell orientation. In this study we consider only dilute suspensions where there is no feedback from cell swimming on the hydrodynamics, and both cell-wall and cell-cell interactions are neglected.

[a)]Corresponding author rbearon@liverpool.ac.uk

I. INTRODUCTION

Phytoplankton are microscopic organisms that live in aquatic environments, and many species swim using either flagella such as *Heterosigma akashiwa*[1] or using cilia such as *Paramecium*[2]. Phytoplankton are important for the environment since they consume carbon dioxide and release oxygen. A certain amount of this carbon is transported to the deep ocean when phytoplankton die which makes the oceans the largest sink of carbon dioxide[3]. There is also interest in using phytoplankton in biotechnology, from the production of biofuels to high-value products, such as β-carotene[4]. Intensive bioreactor culture systems typically consist of arrays of tubes which are pumped or bubbled, and it has been hypothesized that efficient bioreactor designs might aim to make use of the swimming motion of the cells themselves[4].

The swimming behaviour of phytoplankton is determined by a range of internal and external factors. Various species of phytoplankton are gravitactic, that is they swim upwards on average in still fluid which can be beneficial for reaching regions of optimal light. For some species this is due to being bottom-heavy - the centre of gravity for these cells is offset from the centre of buoyancy, and the combination of the effects of gravity with the buoyancy force gives rise to a gravitational torque which serves to reorient the cell allowing it to swim upwards. However, in shear flow the cells may be reoriented from the vertical due to viscous torques[5]. For a vertical pipe containing downwelling fluid, gravitactic cells can accumulate near the centre[6], a phenomenon known as gyrotactic focussing. As recently predicted[7,8], such a modification of the spatial distribution of algae in tubes alters significantly the effective axial transport of cells. Furthermore, the interaction of gyrotactic swimmers with complex flow fields can lead to a rich variety of spatial dynamics[9].

It has been observed that many phytoplankton do not swim in a straight line, rather they undergo helical trajectories[10–12]. Several explanations have been proposed for the ubiquity of helical movement among micro-organisms. Over a century ago, Jennings[13] postulated that the helical trajectory allows an otherwise asymmetric organism to move along a nearly straight trajectory. The term helical klinotaxis was introduced by Crenshaw[10] to demonstrate how organisms can modify their helical motions in order to undergo phototaxis and chemotaxis. Recently Bearon[14] proposed a mechanistic model based on *Heterosigma akashiwa* to generate upwards helical trajectories. Further mechanistic understanding of

how helical swimming motions can be generated was provided by Pak and Lauga[15], who demonstrated how a squirmer model can swim in a helical path if the net force and torque are not parallel. Using the mechanistic model for helical swimming, Bearon[14] showed how in the presence of uniform vertical shear, cells could avoid swimming into regions of downwards flow and retain upwards net transport.

The interaction between cells and the boundaries of a channel is addressed in some studies. Cells swimming near a wall may change their speed[2], or change their trajectories from straight to circular as the case of *E. coli*[16]. The cell-cell interaction may cause changes in the reorientation due to velocity gradients: a flow field created by a cell induces a disturbance flow around the second cell which then influences the velocity and orientation of the first cell[16]. The model we present here is only valid for dilute suspensions where there is no feedback from cell swimming on the hydrodynamics, and both cell-wall and cell-cell interactions are neglected.

Here we consider a mechanistic model describing a generic swimming cell with net force and torque that are not parallel, based on the model of Bearon[14] for the alga *Heterosigma akashiwa*. We consider the transport in channel flow where the shear is non-uniform. In section II we describe the model system of ordinary differential equations describing the cell's orientation. We obtain the stable equilibrium solution for cell orientation as a function of shear strength in section III, and determine analytically the feasibility region for the equilibrium solutions. We also compute numerically the mean horizontal component of swimming orientation for parameters outside the feasibility region. In section IV we numerically compute trajectories for cells in 2D channel flow and demonstrate that, for certain parameter values, cells which are helical swimmers in still fluid may focus away from the centreline of the channel.

II. MODEL

We consider a self-propelled cell which generates a propulsive force in the direction of the unit vector $\mathbf{p}$ and a propulsive torque in the direction of the unit vector $\mathbf{n}$, as depicted in figure 1. The angle between the vectors $\mathbf{p}$ and $\mathbf{n}$ is given by γ which may be non-zero. The propulsive force results in the cell swimming in the direction of $\mathbf{p}$, and the propulsive torque contributes to determining how the vector $\mathbf{p}$ rotates.

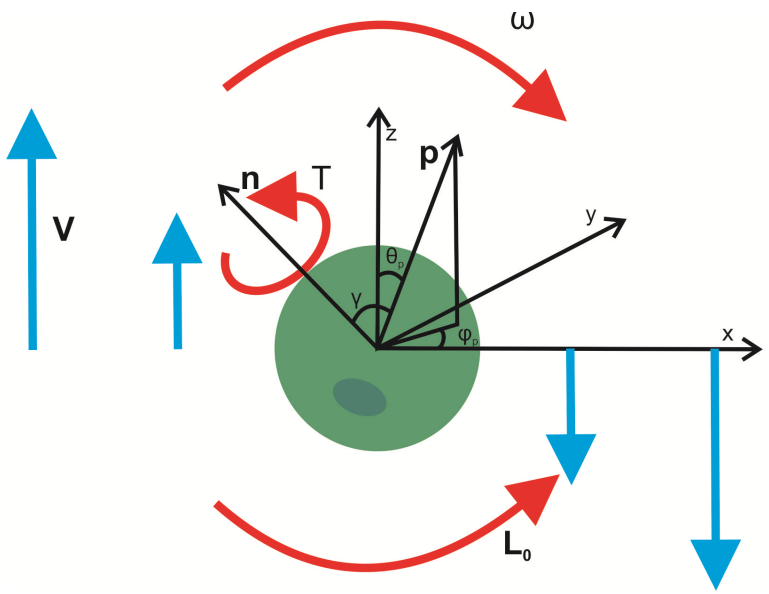

FIG. 1. **Diagram of model organism and co-ordinate system.** The cell orientation is described by two unit vectors, **p** and **n**. The vector **p** is represented in spherical polar co-ordinates by the angles (θ_p, ϕ_p). The angle γ is the (constant) angle between the vectors **p** and **n**. The cell swims in the direction **p** and is situated in vertical shear flow with velocity **V** represented by the vertical arrows. The cell is reorientated due to three torques indicated by the curved arrows: gravity, of magnitude L_0, due to being bottom heavy as indicated by the shaded ellipse; viscosity, in that it is rotated due to the vorticity of the flow, of magnitude ω, and a propulsive torque of magnitude T in the direction of **n**.

To determine how the swimming direction, **p**, rotates, we also consider the gravitational torque acting on the bottom-heavy cell, $\mathbf{L}_g$, and the viscous torque exerted by the surrounding fluid, $\mathbf{L}_v$[5]. Assuming the center of mass to be displaced from the center of buoyancy in the direction $-\mathbf{p}$, the gravitational torque acting on the cell is given by:

$$\mathbf{L}_g = L_o \mathbf{p} \wedge \mathbf{k}, \tag{1}$$

where L_o is the magnitude of the maximum gravitational torque and **k** is a unit vector in the direction of the vertical z-axis. For a spherical cell swimming at low Reynolds number, the viscous torque is given by:

$$\mathbf{L}_v = 8\pi\mu a^3 (\frac{1}{2}\boldsymbol{\omega} - \boldsymbol{\Omega}), \tag{2}$$

where μ is the fluid viscosity, a is the radius of the cell, $\boldsymbol{\omega} = \nabla \wedge \mathbf{V}$ is the vorticity of the fluid with velocity **V**, and $\boldsymbol{\Omega}$ is the angular velocity of the cell. Furthermore, at low

Reynolds number, the total torque on the cell, including the propulsive torque of magnitude T in direction $\mathbf{n}$ will be zero, and so we obtain an expression for the angular velocity of the cell:

$$\mathbf{\Omega} = \frac{1}{2B}\mathbf{p} \wedge \mathbf{k} + R\mathbf{n} + \frac{1}{2}\boldsymbol{\omega}, \tag{3}$$

where $\frac{1}{2B} = \frac{L_o}{8\pi\mu a^3}$ and $R = \frac{T}{8\pi\mu a^3}$ are reorientation rates associated with the gravitational and propulsive torques respectively.

The cell swims according to the following ordinary differential equations[14]:

$$\frac{d\mathbf{x}}{dt} = \mathbf{V} + v\mathbf{p}, \tag{4}$$
$$\frac{d\mathbf{p}}{dt} = \mathbf{\Omega} \wedge \mathbf{p}, \tag{5}$$
$$\frac{d\mathbf{n}}{dt} = \mathbf{\Omega} \wedge \mathbf{n}, \tag{6}$$

where $\mathbf{x}$ is the cell position, $\mathbf{V}$ is the local fluid velocity and $v\mathbf{p}$ is the swimming velocity of the cell.

For simplicity, we consider fluid flow constrained to be in the $x - z$ plane so that the vorticity is given by $\boldsymbol{\omega} = \omega\mathbf{j}$ where $\mathbf{j}$ is a unit vector in the y-direction.

We define the unit vectors $\mathbf{p}$ and $\mathbf{n}$ in spherical polar coordinates, for example $\mathbf{p} = (\sin\theta_p \cos\phi_p, \sin\theta_p \sin\phi_p, \cos\theta_p)$ where θ_p is the angle between $\mathbf{p}$ and the vertical, and ϕ_p is the angle between the projection of $\mathbf{p}$ onto the horizontal $x - y$ plane and the x-axis. The constant angle between $\mathbf{p}$ and $\mathbf{n}$ is defined as $\cos\gamma = \mathbf{p} \cdot \mathbf{n}$.

The vector equations for $d\mathbf{p}/dt$ and $d\mathbf{n}/dt$ can be converted to scalar equations for the variables $\sin\theta_p, \cos\phi_p, \sin\theta_n$ and $\cos\phi_n$[14]. Non-dimensionalising time on $2B$ we obtain the governing equations defining cell orientation:

$$\frac{d\theta_p}{dt} = -\sin\theta_p + \Theta\sin\theta_n \sin(\phi_n - \phi_p) + \Psi\cos\phi_p, \tag{7}$$
$$\sin\theta_p \frac{d\phi_p}{dt} = -\Theta[\sin\theta_n \cos\theta_p \cos(\phi_n - \phi_p) - \cos\theta_n \sin\theta_p] - \Psi\cos\theta_p \sin\phi_p, \tag{8}$$
$$\frac{d\theta_n}{dt} = -\sin\theta_p \cos(\phi_p - \phi_n) + \Psi\cos\phi_n, \tag{9}$$
$$\sin\theta_n \frac{d\phi_n}{dt} = \sin\theta_p \cos\theta_n \sin(\phi_n - \phi_p) - \Psi\cos\theta_n \sin\phi_n, \tag{10}$$

where $\Theta = 2BR$ and $\Psi = B\omega$ are non-dimensional parameters representing the relative strength of the propulsive and viscous torques compared to the gravitational torque. In

section IV we will consider channel flow where the vorticity varies with spatial position, and so the parameter $\Psi = B\omega(\mathbf{x})$ will be a function of the cell position.

As discussed by Bearon [14], in the absence of flow, $\Psi = 0$, this dynamical system describes helical swimming trajectories, and as flow is introduced, the system displays more complex behaviour. Equations (7-10) were solved numerically in Matlab R2014a using the ode45 solver.

III. CELL ORIENTATION AS A FUNCTION OF VORTICITY

To understand the cell dynamics, we first consider equilibrium solutions for the cell orientation, that is consider solutions $\mathbf{p} = \mathbf{p}^e$ and $\mathbf{n} = \mathbf{n}^e$ for constant vectors $\mathbf{p}^e$ and $\mathbf{n}^e$. In this section, we shall assume all parameters are positive. From equations (5-6), if we assume $\mathbf{p}$ and $\mathbf{n}$ are not parallel, we see that the angular velocity, $\mathbf{\Omega}$, given by equation (3), must be zero for the orientation to be at equilibrium.

Taking the dot product of $\mathbf{\Omega} = 0$ with $\mathbf{p}$, and the unit basis vectors $\mathbf{i}, \mathbf{j}$ and $\mathbf{k}$ yields:

$$\begin{aligned} \Theta \cos\gamma + \Psi p_y^e &= 0, \\ p_y^e + \Theta n_x^e &= 0, \\ -p_x^e + \Theta n_y^e + \Psi &= 0, \\ n_z^e &= 0, \end{aligned}$$

which can be solved to find the unit vector $\mathbf{p}^e$.

When the propulsive torque is zero, $\Theta = 0$, provided that $\Psi \leq 1$, cells attain a stable equilibrium orientation given by[5]:

$$\mathbf{p}^e = (\Psi, 0, \sqrt{1-\Psi^2}). \tag{11}$$

Including a propulsive torque, $\Theta \neq 0$, modifies the stable equilibrium orientation to[14]:

$$p_x^e = \Psi - \Theta\sqrt{1 - \left(\frac{\cos\gamma}{\Psi}\right)^2}, \tag{12}$$

$$p_y^e = -\frac{\Theta}{\Psi}\cos\gamma, \tag{13}$$

$$p_z^e = \sqrt{1 - (p_x^e)^2 - (p_y^e)^2}. \tag{14}$$

To determine the feasibility region for this equilibrium solution in $\Theta - \Psi$ parameter space, we require that the components of $\mathbf{p}$ are real. In particular taking $\frac{\cos\gamma}{\Psi} \leq 1$ ensures $p_x^e \in \Re$,

and by substituting equations (12,13) into the condition $(p_x^e)^2 + (p_y^e)^2 < 1$ we obtain a quadratic for Θ:

$$\Psi^2 - 2\Theta\Psi\sqrt{1 - \left(\frac{\cos\gamma}{\Psi}\right)^2} + \Theta^2 < 1 \tag{15}$$

which ensures $p_z^e \in \Re$. To identify where the equilibrium solution is feasible in $\Theta - \Psi$ parameter space, we solve this constraint for Θ to obtain:

$$\Psi \geq \cos\gamma. \tag{16}$$

$$\Psi\sqrt{1 - \left(\frac{\cos\gamma}{\Psi}\right)^2} - \sin\gamma \leq \Theta \leq \Psi\sqrt{1 - \left(\frac{\cos\gamma}{\Psi}\right)^2} + \sin\gamma, \tag{17}$$

or equivalently the second equation can be written as a constraint on Ψ:

$$\sqrt{\Theta^2 - 2\Theta\sin\gamma + 1} \leq \Psi \leq \sqrt{\Theta^2 + 2\Theta\sin\gamma + 1}. \tag{18}$$

In figure 2, these equations demarcate the outer boundary of the region where equilibrium solutions exist. Note that the behaviour for $\Theta = 0$ displays a singular behaviour, in that the lower bound $\Psi \geq \cos\gamma$ is not required to be satisfied for an equilibrium solution to exist. This is because in the absence of a propulsive torque which rotates the cells, an equilibrium solution can be found for arbitrarily small shear rates. However on introducing a propulsive torque, at low shear rates, the cells undergo helical trajectories and so do not have an equilibrium orientation.

We now consider the behaviour of cells outside the region of parameter space where the equilibrium is feasible. In the absence of a propulsive torque, $\Theta = 0$, when the vorticity is sufficiently strong such that the equilibrium is not feasible, $\Psi > 1$, cells tumble with period of oscillation given by $\tau = \frac{2\pi}{\sqrt{\Psi^2-1}}$. Note we correct this expression by a factor of 2 from that derived previously[17] and referenced by Pedley and Kessler[5]. For $\Theta = 0$, the average cell orientation over an oscillation that is constrained to the $x - z$ plane is given by:

$$\overline{p_x} = \frac{1}{T}\int_0^T \sin\theta(t)dt = \frac{1}{T}\int_0^{2\pi} \frac{\sin\theta}{\Psi - \sin\theta}d\theta, \tag{19}$$

$$= \Psi - \sqrt{\Psi^2 - 1}. \tag{20}$$

Note that $\overline{p_x} = 1$ for $\Psi = 1$, which agrees with the equilibrium solution. In figure 3, we compute $\overline{p_x}$ numerically for a range of parameters. In figure 3(b-d) we see that for weak shear (small Ψ), the average value of p_x is the same for helical swimmers as for non-helical swimmers. That is the average value is the same as the equilibrium orientation

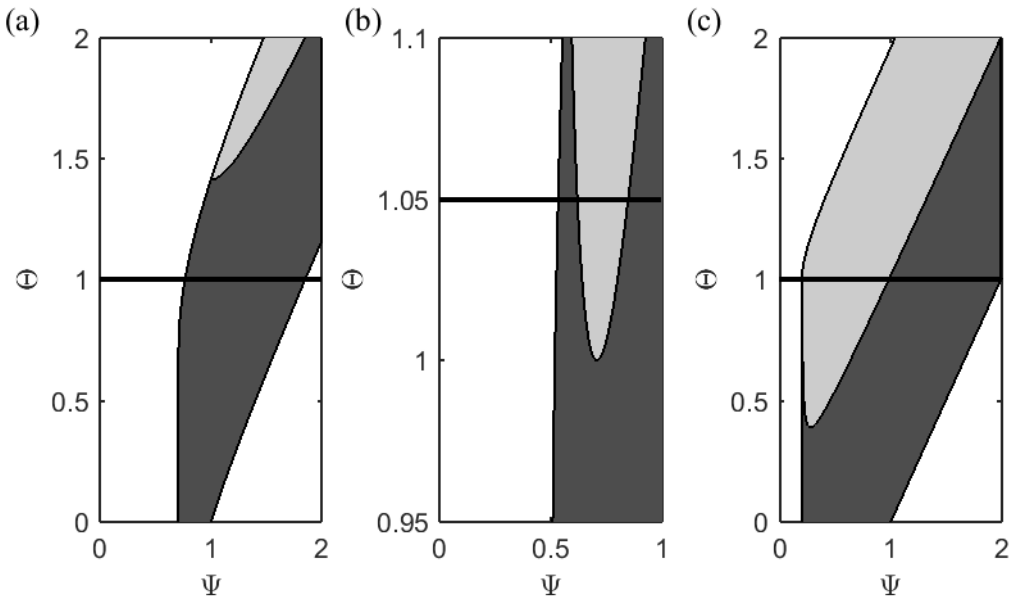

FIG. 2. **Equilibrium feasibility region:** (a) $\gamma = \frac{\pi}{4}$, (b) $\gamma = \frac{\pi}{3}$, and (c) $\gamma = \frac{7\pi}{16}$. The shaded regions indicate where the equilibrium orientation is feasible, with lower and upper curved boundaries given by equation (17) and left-hand vertical boundary given by equation (16). Dark gray regions indicate that $p_x^e > 0$ while light gray regions indicate $p_x^e < 0$. The white region shows the equilibrium is not feasible. Solid horizontal lines indicate feasibility for (a) $\Theta = 1$, (b) $\Theta = 1.05$, and (c) $\Theta = 1$. The axes scales in (b) are chosen to highlight the two values of Ψ where $p_x^e = 0$.

for non-helical gyrotactic swimmers, $\overline{p_x} = \Psi$. However, for helical swimmers, as the shear increases generating a new equilibrium solution, the average value of p_x falls, and can become negative as shown in figure 3(c). In all cases, when the shear increases further and the stable equilibrium solution is lost, the average value of p_x decays to zero (data not shown).

IV. CELL TRAJECTORIES IN CHANNEL FLOW

We now consider Poiseuille flow in a vertical channel between two parallel walls separated by a distance $2L$:

$$\mathbf{V} = \frac{U}{L^2}(x^2 - L^2)\mathbf{k} \tag{21}$$

where U is the flow speed at the center, and $\mathbf{k}$ is a unit vector in $z-$direction. The vorticity of the flow is $\boldsymbol{\omega} = -\frac{2U}{L^2}x\mathbf{j}$. We non-dimensionalise lengths on L, and time on $2B$ as previously,

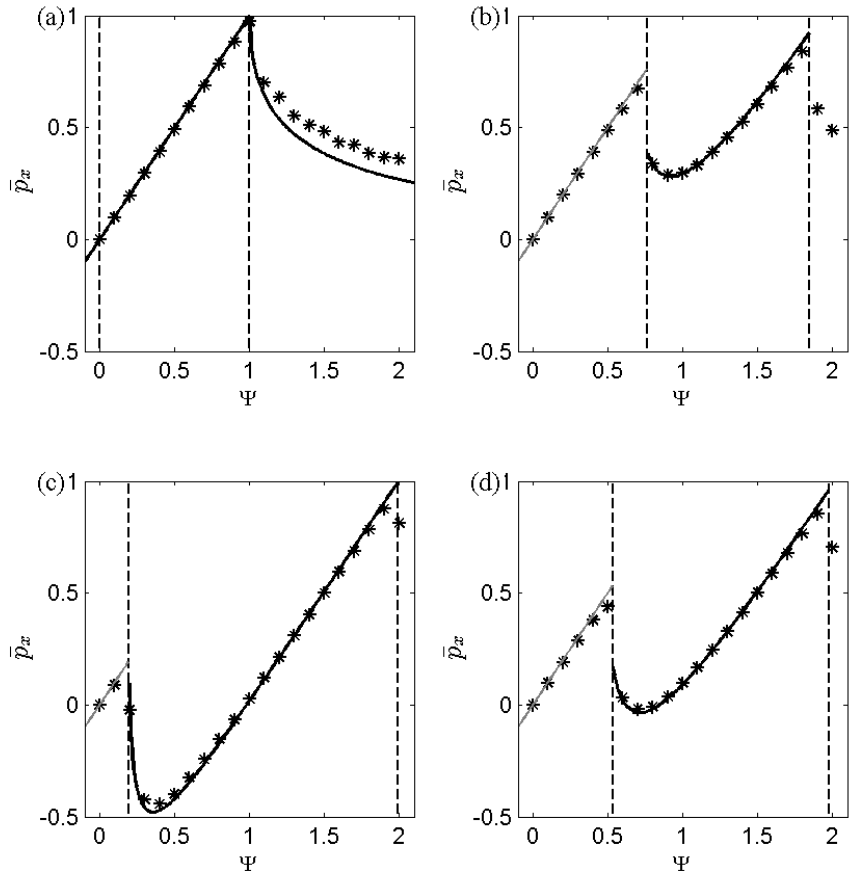

FIG. 3. **Average value of p_x:** Stars indicate the average value for 100 simulations run for 100 time units. The vertical dashed lines are the boundaries of equilibrium feasibility. (a) $\Theta = 0$. (b) $\Theta = 1$, $\gamma = \frac{\pi}{4}$. (c) $\Theta = 1$, $\gamma = \frac{7\pi}{16}$ (d) $\Theta = 1.05$, $\gamma = \frac{\pi}{3}$. In (a) the solid line is the analytical average for $\Theta = 0$ given by equation (20) for $\Psi > 1$ and the equilibrium value for $\Psi < 1$, given by $p_x^e = \Psi$. In (b-d) the black solid lines are the equilibrium value given by equation (12) for values of Ψ where the equilibrium is feasible. The grey lines are the $\Theta = 0$ equilibrium value, $p_x^e = \Psi$.

so as to obtain an expression for Ψ, the non-dimensional measure of the viscous torque:

$$\Psi = -\Psi_{max} x, \tag{22}$$

where $\Psi_{max} = \frac{2BU}{L}$. With respect to non-dimensional variables, the governing equation for cell position, equation (4) is given by:

$$\frac{d\mathbf{x}}{dt} = \Psi_{max}(x^2 - 1)\mathbf{k} + \nu\mathbf{p} \tag{23}$$

where $\nu = \frac{2Bv}{L}$ is the non-dimensional swimming speed which we take equal to 0.1 in the simulations. We simulated the trajectories of cells swimming in the Poiseuille flow, by solving equation (23) coupled with the equations for orientation (7-10) with the shear parameter $\Psi(x)$ given by equation (22). We imposed absorbing boundary conditions on the channel boundaries such that cells that reach the wall remain there.

If there is no propulsive torque, $\Theta = 0$, cells are focused in the centre of channel as found by Kessler [6] and as shown in figures 4a and 5a. This can be explained by making the assumption that the average cell orientation as a function of position is approximately that given by the average cell orientation for the shear rate at that position as depicted in figure 3. The equilibrium swimming direction, given by equation (11), has horizontal component $p_x^e = \Psi$, where $\Psi = -\Psi_{max}x$, and the mean horizontal component of swimming direction for tumbling cells, given by equation (20), is $\overline{p}_x = \Psi - \sqrt{\Psi^2 - 1}$. When $|\Psi| < 1$, corresponding to the inner region $|x| < 1/\Psi_{max}$, we have an equilibrium swimming direction that is towards the centre of the channel. When $|\Psi| > 1$, corresponding to the outer region where $|x| > 1/\Psi_{max}$, the mean value of p_x is also towards the centre of the channel.

When the propulsive torque is non-zero, $\Theta \neq 0$, we can identify three distinct regions in the channel. Again, we make the assumption that cell orientation can be described by the local shear rate, and noting that Ψ is proportional to x, we can interpret figure 3 as a plot of the average value of p_x as a function of position, x. In the central region cells swim in helical paths because the viscous torque is insufficient to balance the propulsive torque and generate a stable equilibrium swimming orientation. From figure 2 and equations (16) and (18) we see this occurs when

$$|x| \leq \frac{1}{\Psi_{max}} \max\{\cos\gamma, \sqrt{\Theta^2 - 2\Theta\sin\gamma + 1}\} \tag{24}$$

Outside this region, within the region of $\Theta - \Psi$ parameter space where equilibrium solutions are feasible, cells attain an equilibrium orientation given by equations (12-14). Finally, near the walls, if the shear is sufficiently strong the viscous torque will cause the cells to tumble. From figure 2 and equation (18) we see this occurs when

$$|x| \geq \frac{1}{\Psi_{max}} \sqrt{\Theta^2 + 2\Theta\sin\gamma + 1}. \tag{25}$$

As a specific example, for the parameters $\Psi_{max} = 2$, $\gamma = \pi/4$, $\Theta = 1$, solving equation (18) for $|x|$ we determine that cells may attain an equilibrium orientation when $0.382 \leq$

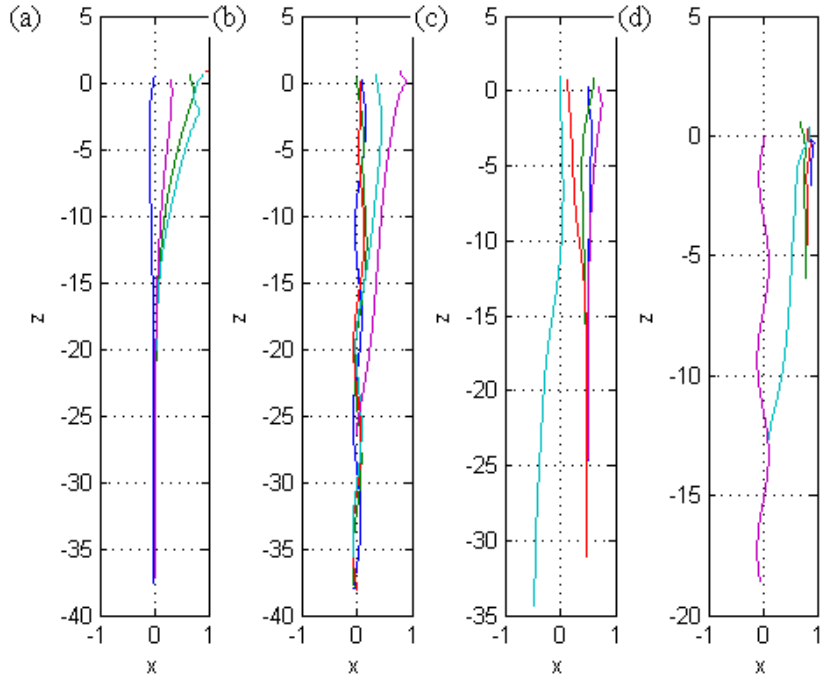

FIG. 4. **Swimming trajectories in a vertical channel**: Example trajectories of duration 20 time units with parameters $\Psi_{max} = 2$ and (a) $\Theta = 0$, (b) $\Theta = 1$, $\gamma = \frac{\pi}{4}$, (c) $\Theta = 1$, $\gamma = \frac{7\pi}{16}$, and (d) $\Theta = 1.05$, $\gamma = \frac{\pi}{3}$.

$|x| \leq 0.923$. This can also be seen from the feasibility region in figure 2a. Closer to the centre of the channel, cells retain helical swimming motion, and near the walls, cells will tumble. However, for these parameters, from figure 3b, the average swimming direction computed for a fixed shear rate is towards the centre throughout the channel and we thus see focussing towards the centreline as shown in figure 4b and 5b.

Because of the effect of Θ on the nature of the equilibrium solutions, the focussing behaviour may change qualitatively, and we can find focussing away from the centreline as shown in figures 4c and 5c. This occurs because there is a location away from the centreline where the horizontal component of swimming is zero, as shown in figure 3c. From equation (12), solving for $p_x^e = 0$ gives:

$$|x| = \frac{1}{\Psi_{max}} \sqrt{\frac{\Theta^2 \pm \Theta\sqrt{\Theta^2 - 4\cos^2\gamma}}{2}}. \tag{26}$$

For example, for the parameters $\Psi_{max} = 2$, $\gamma = 7\pi/16$, we find that equilibria are feasible for $0.0980 < |x| < 0.9952$ and $p_x^e = 0$ when $|x| = 0.099$ and $|x| = 0.49$. For these parameters,

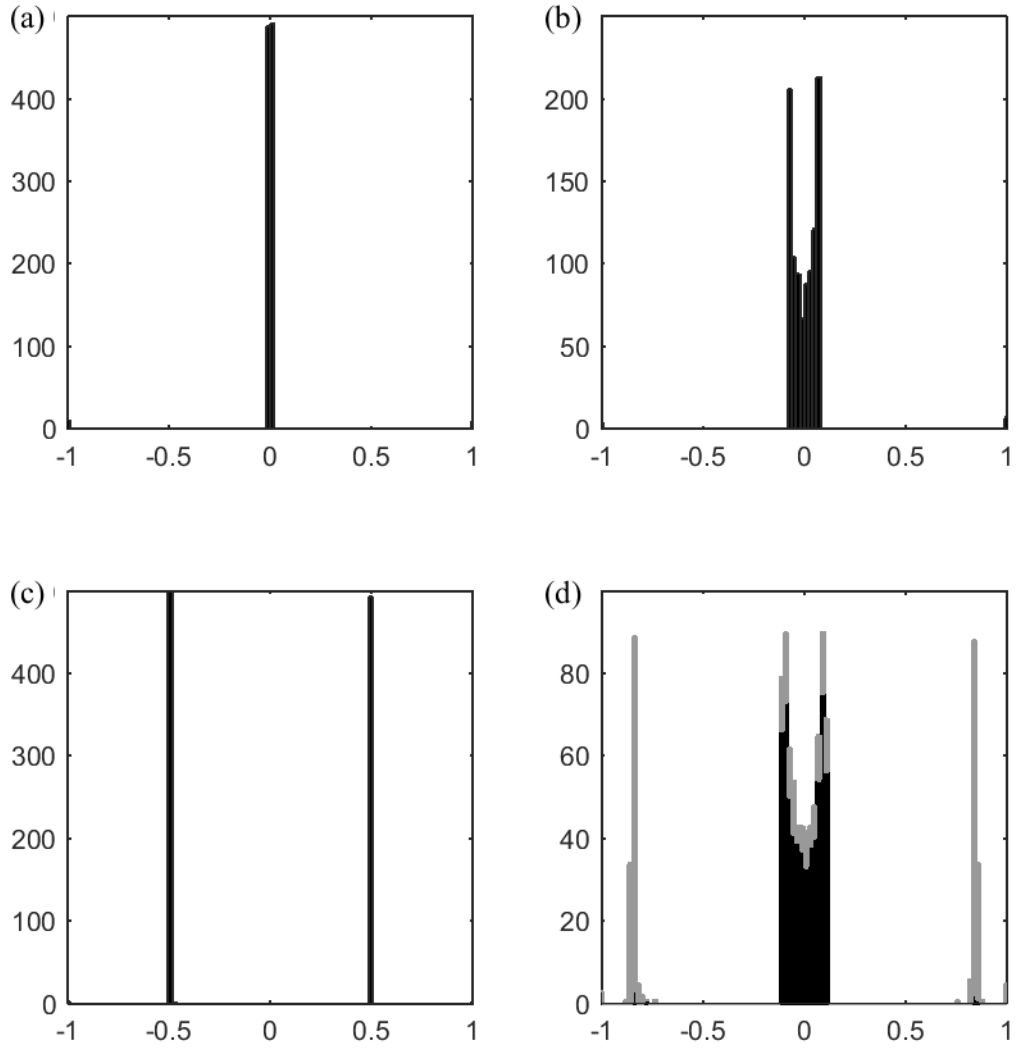

FIG. 5. **Distribution of cells across the channel:** Horizontal position after 100 time units of 1000 cells initially uniformly distributed across the channel with parameters (a) $\Theta = 0$,$\Psi_{max} = 2$; (b) $\Theta = 1$, $\gamma = \frac{\pi}{4}$, $\Psi_{max} = 2$; c) $\Theta = 1$, $\gamma = \frac{7\pi}{16}$, $\Psi_{max} = 2$; (d) $\Theta = 1.05$, $\gamma = \frac{\pi}{3}$, $\Psi_{max} = 1$. In (d) grey indicates cells which had initial position $|x| > 0.61$ and black indicates cells which had initial position $|x| < 0.61$.

when $0.099 < |x| < 0.49$ we see the equilibrium orientation is away from the centreline and when $0.49 < |x| < 0.995$ the equilibrium orientation is towards the centreline and we therefore see focussing at the interface, $|x| = 0.49$ where the horizontal component of

swimming is zero.

As a final example, we select parameters where the roots of $p_x^e = 0$ are visually distinct from the feasibility boundary; $\Psi_{max} = 1$, $\gamma = \pi/3$, $\Theta = 1.05$ (see figures 2b, 3d). We find that equilibria are feasible for $0.53 \leq |x| \leq 1.98$ and $p_x^e = 0$ when $|x| = 0.61$ or $|x| = 0.84$. By examining the sign of the average horizontal component of orientation, we predict that cells positioned within the central region $|x| < 0.61$ swim towards the centreline while cells positioned outside this region swim towards the location $|x| = 0.84$. Therefore, accumulation away from the center can be noticed in figures 4d and 5d. Furthermore, in figure 5d we see how cells with initial position $|x| < 0.61$ tend to accumulate at the centreline whilst some cells with initial position closer to the walls are focussed towards the point $|x| = 0.84$.

V. DISCUSSION

We have analyzed a simple mechanistic model for gravitactic organisms propelled by a propulsive force and a propulsive torque which are not parallel. The model generates helical swimming trajectories if the shear is sufficiently weak, but a stable equilibrium orientation arises at moderate values of shear representing a balance between the viscous torque, gravitational torque and propulsive torque. We have derived analytic expressions for the feasibility of the equilibrium orientation states as functions of the model parameters. Gyrotactic non-helical swimmers are known to focus in the centre of channel flow, at the point where the horizontal component of swimming and the shear are zero. We showed this is also true when the propulsive torque is not too strong; although helical swimming in the central region resulted in a spread in the distribution. We also discovered that for certain parameter values, cells focussed away from the centre, as the point where the horizontal component of swimming is zero can be at a different location from the position of zero shear. We were able to explain the results of the numerical simulations by comparison with the equilibrium solutions for orientation.

The model leads to some experimentally testable hypotheses concerning how cells aggregate in channel or pipe flow. Specifically to validate our predictions of gyrotactic focussing away from the centre of the tube, firstly the biological swimming parameters would need to be extracted from trajectory data in still fluid (e.g. data from Gurarie, Grünbaum, and Nishizaki [11] and Crenshaw [10]), and then experiments would need to be designed with tubes

of the appropriate dimension and flow of the appropriate range of speeds. Designing experiments to analyze individual swimming trajectories in flow is challenging[18,19], but the predictions from this model are robust to population-level experiments which may be more feasible to implement[6,9].

Throughout the paper we have assumed the cell's motion is deterministic, however in reality there is randomness in the cell trajectories. For gyrotactic swimmers, this has been modelled by a Smoluchowski equation for the probability density function $f(\mathbf{p}, \mathbf{x}, t)$ for cell orientation and position[20,21]:

$$\frac{\partial f}{\partial t} + \nabla_{\mathbf{x}} \cdot (\dot{\mathbf{x}} f - D \nabla_{\mathbf{x}} f) + \nabla_{\mathbf{p}} \cdot (\dot{\mathbf{p}} f - d_r \nabla_{\mathbf{p}} f) = 0, \tag{27}$$

where $\dot{\mathbf{x}}$ represents the deterministic spatial transport given by equation (4), $\dot{\mathbf{p}}$ is the determinstic rate of change in orientation determined from equation (3), and D and d_r are the translational and rotational diffusion coefficients respectively. Previously it has been shown that the dominant contribution to diffusion is due to fluctuations in the cell's swimming direction as represented by the rotational diffusion coefficient d_r. This general formulation for the distribution function has been recently reviewed for example by Saintillan and Shelley[22]. Averaging the Smoluchowski equation to obtain population-level models describing dispersion in a pipe will require further theoretical developments[23,24]. The corresponding Smoluchowski equation for biaxial helical swimmers will be more complex because of the extra degree of freedom associated with the vector $\mathbf{n}$ associated with the propulsive torque. Further simulations and experiments are required to understand what the implications are for the spatial distribution of helical swimmers in more complex flow fields. We note that in explaining the numerical results of this paper, we took the cell's orientation to be at equilibrium; this quasi-steady assumption may not hold in flows where cells experience rapidly changing shear.

We have here demonstrated how fluid forces can significantly modify swimming trajectories and the resultant spatial distribution of cells. In the situation we have considered of gyrotactic focussing in a dilute suspension we rarely observed cells encountering the walls because they tended to swim away from the wall towards the centre of the pipe, and thus we do not think interactions with the walls plays an important role. Furthermore, whilst we have neglected cell-cell interactions, which would become important according to our deterministic predictions of focussing along a vertical line, we anticipate that the first cor-

rection that is important to make in our model is to include randomness in cell swimming orientation which would cause the cells to spread diffusively around this vertical focal line.

The results presented here are relevant to studies which aim to employ the microorganism swimming mechanism in bioreactor design[4]. Cells can typically be cultured in liquid cultures to average volume fractions of only 10^{-3} suggesting that the model proposed here for dilute suspensions is realizable. It has previously been shown how the transport of active swimmers in vertical pipes is very different to passive solutes, because of their non-uniform cross-sectional distribution. For example, gyrotactic cells focus in the central, fastest moving, region of the pipe and so are transported along the pipe axis more rapidly than passive solutes. However these models have not considered helical swimmers, which we have here shown may have a very different cross-sectional distribution. Our model predicts that helical swimmers which focus away from the centre would have a reduced transport rate compared to non-helical swimmers.

The area of active suspensions contains rich problems in fluid dynamics. Bioconvection patterns are commonly observed in laboratory cultures of phytoplankton[5] and found in natural environments[25]. At higher volume fractions, the swimming stresses exerted on the fluid can drive fluid motions on spatial and temporal scales much larger than the individual cells[26]. Furthermore particle-particle hydrodynamic interactions can lead to strong boundary accumulations[27]. It is likely to be interesting to investigate how the forces generated by the swimmers couple back onto the fluid dynamics leading to yet more complex dynamics.

ACKNOWLEDGMENTS

M. S. A. is grateful to King Khalid University for financially sponsoring his postgraduate studies at the University of Liverpool.

REFERENCES

[1]Y. Hara and M. Chihara, "Morphology, ultrastructure and taxonomy of the raphidophycean alga *Heterosigma akashiwo*," Bot. Mag. Tokyo **100**, 151–163 (1987).

[2]C. Brennen and H. Winet, "Fluid mechanics of propulsion by cilia and flagella," Annu. Rev. Fluid Mech. **9**, 339–398 (1977).

[3]J. A. Raven and P. G. Falkowski, "Oceanic sinks for atmospheric CO_2," Plant, Cell & Environment **22**, 741–755 (1999).

[4]M. A. Bees and O. A. Croze, "Mathematics for streamlined biofuel production from unicellular algae," Biofuels **5**, 53–65 (2014).

[5]T. J. Pedley and J. O. Kessler, "Hydrodynamic phenomena in suspensions of swimming microorganisms," Annu. Rev. Fluid Mech. **24**, 313–358 (1992).

[6]J. O. Kessler, "Hydrodynamic focusing of motile algal cells," Nature **313**, 218–220 (1985).

[7]M. A. Bees and O. A. Croze, "Dispersion of biased swimming micro-organisms in a fluid flowing through a tube," Proc. R. Soc., London Ser. B **466**, 2057–2077 (2010).

[8]R. N. Bearon, M. A. Bees, and O. A. Croze, "Biased swimming cells do not disperse in pipes as tracers: a population model based on microscale behaviour," Phys. Fluids **24**, 121902 (2012).

[9]W. M. Durham, E. Climent, M. Barry, F. De Lillo, G. Boffetta, M. Cencini, and R. Stocker, "Turbulence drives microscale patches of motile phytoplankton," Nat. Commun. **4** (2013).

[10]H. C. Crenshaw, "A new look at locomotion in microorganisms: rotating and translating," Am. Zool. **36**, 608–618 (1996).

[11]E. Gurarie, D. Grünbaum, and M. T. Nishizaki, "Estimating 3D movements from 2D observations using a continuous model of helical swimming," B. Math. Biol. **73**, 1358–1377 (2011).

[12]D. E. Boakes, E. A. Codling, G. J. Thorn, and M. Steinke, "Analysis and modelling of swimming behaviour in *Oxyrrhis marina*," J. Plankton Res. **33**, 641–649 (2010).

[13]H. S. Jennings, "On the significance of the spiral swimming of organisms," Am. Nat. **35**, 369–378 (1901).

[14]R. N. Bearon, "Helical swimming can provide robust upwards transport for gravitactic single-cell algae; a mechanistic model," J. Math. Biol. **66**, 1341–1359 (2013).

[15]O. S. Pak and E. Lauga, "Generalized squirming motion of a sphere," J. Eng. Math. **88**, 1–28 (2014).

[16]E. Lauga and T. R. Powers, "The hydrodynamics of swimming microorganisms," Rep Prog Phys **72**, 096601 (2009).

[17]W. F. Hall and S. N. Busenberg, "Viscosity of magnetic suspensions," J. Chem. Phys. **51**, 137–144 (1969).

[18]L. Karp-Boss, E. Boss, and P. Jumars, "Motion of dinoflagellates in a simple shear flow,"

Limnol. Oceanogr. **45**, 1594–1602 (2000).

[19]W. M. Durham, J. O. Kessler, and R. Stocker, "Disruption of vertical motility by shear triggers formation of thin phytoplankton layers," Science **323**, 1067–1070 (2009).

[20]N. A. Hill and M. A. Bees, "Taylor dispersion of gyrotactic swimming micro-organisms in a linear flow," Phys. Fluids **14**, 2598 – 2605 (2002).

[21]A. Manela and I. Frankel, "Generalized Taylor dispersion in suspensions of gyrotactic swimming micro-organisms," J. Fluid Mech. **490**, 99 – 127 (2003).

[22]D. Saintillan and M. J. Shelley, "Active suspensions and their nonlinear models," Comptes Rendus Physique **14**, 497–517 (2013).

[23]B. Ezhilan and D. Saintillan, "Transport of a dilute active suspension in pressure-driven channel flow," J. Fluid Mech. **777**, 482–522 (2015).

[24]R. N. Bearon and A. L. Hazel, "The trapping in high-shear regions of slender bacteria undergoing chemotaxis in a channel," J. Fluid Mech. **771**, 1–13 (2015).

[25]R. N. Bearon and D. Grünbaum, "Bioconvection in a stratified environment: Experiments and theory," Phys. Fluids **18**, 127102 (2006).

[26]E. Lushi, H. Wioland, and R. E. Goldstein, "Fluid flows created by swimming bacteria drive self-organization in confined suspensions," Proc. Nat. Acad. Sci. USA **111**, 9733–9738 (2014).

[27]J. P. Hernández-Ortiz, P. T. Underhill, and M. D. Graham, "Dynamics of confined suspensions of swimming particles," J. Phys. Condens. Matter **21**, 204107 (2009).